

## Testing the monogamy relations via rank-2 mixtures

Eylee Jung<sup>1</sup> and DaeKil Park<sup>1,2</sup>

<sup>1</sup>Department of Electronic Engineering, Kyungnam University, Changwon 631-701, Korea

<sup>2</sup>Department of Physics, Kyungnam University, Changwon 631-701, Korea

(Received 4 July 2016; published 20 October 2016)

We introduce two tangle-based four-party entanglement measures  $t_1$  and  $t_2$ , and two negativity-based measures  $n_1$  and  $n_2$ , which are derived from the monogamy relations. These measures are computed for three four-qubit maximally entangled and  $W$  states explicitly. We also compute these measures for the rank-2 mixture  $\rho_4 = p|\text{GHZ}_4\rangle\langle\text{GHZ}_4| + (1-p)|W_4\rangle\langle W_4|$  by finding the corresponding optimal decompositions. It turns out that  $t_1(\rho_4)$  is trivial and the corresponding optimal decomposition is equal to the spectral decomposition. Probably, this triviality is a sign of the fact that the corresponding monogamy inequality is not sufficiently tight. We fail to compute  $t_2(\rho_4)$  due to the difficulty in the calculation of the residual entanglement. The negativity-based measures  $n_1(\rho_4)$  and  $n_2(\rho_4)$  are explicitly computed and the corresponding optimal decompositions are also derived explicitly.

DOI: 10.1103/PhysRevA.94.042330

### I. INTRODUCTION

Research into the entanglement of quantum states has a long history from the very beginning of quantum mechanics [1,2]. At that time the main motivation for the study of entanglement was purely theoretical. It was to explore the nonlocal properties of quantum mechanics. Recent considerable attention to quantum entanglement [3,4] has both theoretical and practical aspects. While the former is for a deeper understanding of quantum information theories, the latter is for developing quantum technology. As shown for last two decades quantum entanglement plays a central role in quantum teleportation [5], superdense coding [6], quantum cloning [7], and quantum cryptography [8,9]. It is also quantum entanglement that makes a quantum computer<sup>1</sup> outperform a classical one [11]. Thus, it is very important to understand how to quantify and how to characterize the entanglement. Still, however, this issue is not completely understood.

For a bipartite quantum system, many entanglement measures were constructed before such as distillable entanglement [12], entanglement of formation (EOF) [12], and relative entropy of entanglement (REE) [13,14]. Among them<sup>2</sup> the closed formula for the analytic computation of EOF for states of two qubits was found in Ref. [16] via the concurrence  $\mathcal{C}$  as

$$E_F(\mathcal{C}) = h\left(\frac{1 + \sqrt{1 - \mathcal{C}^2}}{2}\right), \quad (1.1)$$

where  $h(x)$  is a binary entropy function  $h(x) = -x \ln x - (1-x) \ln(1-x)$ . For two-qubit pure state  $|\psi\rangle_{AB} = \psi_{ij}|ij\rangle_{AB}$  with  $(i, j = 0, 1)$ , the concurrence  $\mathcal{C}_{A|B}$  between party A and party B is given by

$$\mathcal{C}_{A|B} = |\epsilon_{i_1 i_2} \epsilon_{j_1 j_2} \psi_{i_1 j_1} \psi_{i_2 j_2}| = 2|\psi_{00}\psi_{11} - \psi_{01}\psi_{10}|, \quad (1.2)$$

<sup>1</sup>The current status of quantum computer technology was reviewed in Ref. [10].

<sup>2</sup>Although there are a lot of attempts to derive the closed formula for REE, we still do not know how to compute the REE for the arbitrary two-qubit mixtures except in rare cases [15].

where the Einstein convention is understood and  $\epsilon_{\mu\nu}$  is an antisymmetric tensor. For two-qubit mixed state  $\rho_{AB}$  the concurrence  $\mathcal{C}_{A|B}(\rho)$  can be computed by  $\mathcal{C}_{A|B} = \max(\lambda_1 - \lambda_2 - \lambda_3 - \lambda_4, 0)$ , where  $\{\lambda_1^2, \lambda_2^2, \lambda_3^2, \lambda_4^2\}$  are eigenvalues of positive operator  $\rho(\sigma_y \otimes \sigma_y)\rho^*(\sigma_y \otimes \sigma_y)$  with decreasing order. Thus, one can compute the EOF for all two-qubit states in principle.

Generalization to the multipartite entanglement is a highly important and challenging issue in the context of quantum information theories. A seminal step toward this goal was initiated in Ref. [17] by examining the three-qubit pure states. The authors in Ref. [17] have shown analytically the monogamy relation

$$\mathcal{C}_{q_1|(q_2 q_3)}^2 \geq \mathcal{C}_{q_1|q_2}^2 + \mathcal{C}_{q_1|q_3}^2. \quad (1.3)$$

This relation implies that the entanglement (measured by the squared concurrence) between  $q_1$  and the remaining parties always exceeds the entanglement between  $q_1$  and  $q_2$  plus the entanglement between  $q_1$  and  $q_3$ . This means that if  $q_1$  and  $q_2$  are maximally entangled, the whole system cannot have the tripartite entanglement. The inequality (1.3) is strong in the sense that the three-qubit  $W$  state [18]

$$|W_3\rangle = \frac{1}{\sqrt{3}}(|001\rangle + |010\rangle + |100\rangle) \quad (1.4)$$

saturates the inequality. Moreover, for three-qubit pure state  $|\psi\rangle_{ABC} = \psi_{ijk}|ijk\rangle_{ABC}$  the leftover in the inequality

$$\tau_{A|B|C} = \mathcal{C}_{A|(BC)}^2 - (\mathcal{C}_{A|B}^2 + \mathcal{C}_{A|C}^2), \quad (1.5)$$

which we will call the residual entanglement,<sup>3</sup> has the following two expressions:

$$\begin{aligned} \tau_{A|B|C} &= |2\epsilon_{i_1 i_2} \epsilon_{i_3 i_4} \epsilon_{j_1 j_2} \epsilon_{j_3 j_4} \epsilon_{k_1 k_3} \epsilon_{k_2 k_4} \psi_{i_1 j_1 k_1} \psi_{i_2 j_2 k_2} \psi_{i_3 j_3 k_3} \psi_{i_4 j_4 k_4}| \\ &= 4|d_1 - 2d_2 + 4d_3|, \end{aligned} \quad (1.6)$$

where

$$d_1 = \psi_{000}^2 \psi_{111}^2 + \psi_{001}^2 \psi_{110}^2 + \psi_{010}^2 \psi_{101}^2 + \psi_{100}^2 \psi_{011}^2,$$

<sup>3</sup>In this paper  $\sqrt{\tau_{A|B|C}}$  is called the three-tangle.

$$\begin{aligned} d_2 &= \psi_{000}\psi_{111}\psi_{011}\psi_{100} + \psi_{000}\psi_{111}\psi_{101}\psi_{010} \\ &\quad + \psi_{000}\psi_{111}\psi_{110}\psi_{001} + \psi_{011}\psi_{100}\psi_{101}\psi_{010} \\ &\quad + \psi_{011}\psi_{100}\psi_{110}\psi_{001} + \psi_{101}\psi_{010}\psi_{110}\psi_{001}, \\ d_3 &= \psi_{000}\psi_{110}\psi_{101}\psi_{011} + \psi_{111}\psi_{001}\psi_{010}\psi_{100}. \end{aligned} \quad (1.7)$$

From the first expression one can show that  $\tau_{A|B|C}$  is invariant under a stochastic local operation and classical communication (SLOCC) [19]. From the second expression one can show that  $\tau_{A|B|C}$  is invariant under the qubit permutation. It was also shown in Ref. [17] that  $\tau_{A|B|C}$  is an entanglement monotone. Thus, the residual entanglement (or three-tangle) can play a role as an important measure for the genuine three-way entanglement.

By making use of Eq. (1.6) one can compute the residual entanglement of all three-qubit pure states. For a mixed state the residual entanglement is usually defined as a convex roof method [12,20]

$$\tau_{A|B|C}(\rho) = \min \sum_i p_i \tau_{A|B|C}(|\psi_i\rangle\langle\psi_i|), \quad (1.8)$$

where the minimum is taken over all possible ensembles of pure states. The ensemble corresponding to the minimum of  $\tau_{A|B|C}$  is called optimal decomposition. For the given three-qubit mixed state it is highly difficult, in general, to find its optimal decomposition except in very rare cases [21].<sup>4</sup>

In order to find the entanglement measures in the multipartite system, there are two different approaches. The first approach is to find the invariant monotones under the SLOCC transformation. As Ref. [24] has shown, any linearly homogeneous positive function of a pure state that is invariant under determinant 1 SLOCC operations is an entanglement monotone. Thus, the concurrence  $C_{A|B}$  and the three-tangle  $\sqrt{\tau_{A|B|C}}$  are monotones. It is also possible to construct the SLOCC-invariant monotones in the higher-qubit systems. In the higher-qubit systems, however, there are many independent monotones, because the number of independent SLOCC-invariant monotones is equal to the degrees of freedom of a pure quantum state minus the degrees of freedom induced by the determinant 1 SLOCC operations. For example, there are  $2(2^n - 1) - 6n$  independent monotones in the  $n$ -qubit system. Thus, in the four-qubit system there are six invariant monotones. Among them, it was shown in Ref. [25] by making use of the antilinearity [20] that there are the following three independent monotones which measure the true four-way entanglement:

$$\begin{aligned} \mathcal{F}_1^{(4)} &= (\sigma_\mu \sigma_\nu \sigma_2 \sigma_2) \bullet (\sigma^\mu \sigma_2 \sigma_\lambda \sigma_2) \bullet (\sigma_2 \sigma^\nu \sigma^\lambda \sigma_2), \\ \mathcal{F}_2^{(4)} &= (\sigma_\mu \sigma_\nu \sigma_2 \sigma_2) \bullet (\sigma^\mu \sigma_2 \sigma_\lambda \sigma_2) \bullet (\sigma_2 \sigma^\nu \sigma_2 \sigma_\tau) \bullet (\sigma_2 \sigma_2 \sigma^\lambda \sigma^\tau), \\ \mathcal{F}_3^{(4)} &= \frac{1}{2} (\sigma_\mu \sigma_\nu \sigma_2 \sigma_2) \bullet (\sigma^\mu \sigma^\nu \sigma_2 \sigma_2) \bullet (\sigma_\rho \sigma_2 \sigma_\tau \sigma_2) \\ &\quad \bullet (\sigma^\rho \sigma_2 \sigma^\tau \sigma_2) \bullet (\sigma_\kappa \sigma_2 \sigma_2 \sigma_\lambda) \bullet (\sigma^\kappa \sigma_2 \sigma_2 \sigma^\lambda), \end{aligned} \quad (1.9)$$

where  $\sigma_0 = \mathbb{1}_2$ ,  $\sigma_1 = \sigma_x$ ,  $\sigma_2 = \sigma_y$ ,  $\sigma_3 = \sigma_z$ , and the Einstein convention is introduced with a metric  $g^{\mu\nu} = \text{diag}\{-1, 1, 0, 1\}$ .

TABLE I.  $\mathcal{F}_1^{(4)}$ ,  $\mathcal{F}_2^{(4)}$ , and  $\mathcal{F}_3^{(4)}$  of the maximally entangled and  $\tilde{W}_4$  states.

	$\mathcal{F}_1^{(4)}$	$\mathcal{F}_2^{(4)}$	$\mathcal{F}_3^{(4)}$
$ \Phi_1\rangle$	1	1	$\frac{1}{2}$
$ \Phi_2\rangle$	$\frac{8}{9}$	0	0
$ \Phi_3\rangle$	0	0	1
$ \tilde{W}_4\rangle$	0	0	0

The solid dot in Eqs. (1.9) is defined as follows. Let  $|\psi\rangle$  be a four-qubit state. Then, for example,  $\mathcal{F}_1^{(4)}$  of  $|\psi\rangle$  is defined as

$$\begin{aligned} \mathcal{F}_1^{(4)}(\psi) &= |\langle\psi^*|\sigma_\mu \otimes \sigma_\nu \otimes \sigma_2 \otimes \sigma_2|\psi\rangle\langle\psi^*|\sigma^\mu \otimes \sigma_2 \otimes \sigma_\lambda \\ &\quad \otimes \sigma_2|\psi\rangle\langle\psi^*|\sigma_2 \otimes \sigma^\nu \otimes \sigma^\lambda \otimes \sigma_2|\psi\rangle|. \end{aligned} \quad (1.10)$$

Other measures can be computed similarly. Furthermore, it was shown in Ref. [26] that there are the following three maximally entangled states in the four-qubit system:

$$\begin{aligned} |\text{GHZ}_4\rangle &= \frac{1}{\sqrt{2}}(|0000\rangle + |1111\rangle), \\ |\Phi_2\rangle &= \frac{1}{\sqrt{6}}(\sqrt{2}|1111\rangle + |1000\rangle + |0100\rangle + |0010\rangle + |0001\rangle), \\ |\Phi_3\rangle &= \frac{1}{2}(|1111\rangle + |1100\rangle + |0010\rangle + |0001\rangle). \end{aligned} \quad (1.11)$$

The measures  $\mathcal{F}_1^{(4)}$ ,  $\mathcal{F}_2^{(4)}$ , and  $\mathcal{F}_3^{(4)}$  of  $|\text{GHZ}_4\rangle$ ,  $|\Phi_2\rangle$ , and  $|\Phi_3\rangle$ , and

$$|\tilde{W}_4\rangle = \frac{1}{2}(|0111\rangle + |1011\rangle + |1101\rangle + |1110\rangle) \quad (1.12)$$

are summarized in Table I. Recently,  $\mathcal{F}_j^{(4)}$  ( $j = 1, 2, 3$ ) and the corresponding linear monotones<sup>5</sup>  $\mathcal{G}_j^{(4)}$  ( $j = 1, 2, 3$ ) for the rank-2 mixtures consisting of one of the maximally entangled states and  $|\tilde{W}_4\rangle$  are explicitly computed [27].

The second approach is to find the monogamy relations in the multipartite system. As Ref. [28] has shown analytically, the monogamy relation

$$\mathcal{C}_{q_1|q_2\cdots q_n}^2 \geq \mathcal{C}_{q_1|q_2}^2 + \mathcal{C}_{q_1|q_3}^2 + \cdots + \mathcal{C}_{q_1|q_n}^2 \quad (1.13)$$

holds in the  $n$ -qubit pure-state system. However, the leftover of Eq. (1.13) is not entanglement monotone. The authors in Refs. [29,30] conjectured that in the four-qubit system the quantity

$$t_1 = \frac{\pi_A + \pi_B + \pi_C + \pi_D}{4} \quad (1.14)$$

is a monotone, where  $\pi_A = \mathcal{C}_{A|(BCD)}^2 - (\mathcal{C}_{A|B}^2 + \mathcal{C}_{A|C}^2 + \mathcal{C}_{A|D}^2)$  and other ones are obtained by changing the focusing qubit. Even though  $t_1$  might be an entanglement monotone, it is obvious that it is not a true four-way measure because it detects the three-way entanglement. For example,  $t_1(g_3) = 3/4$ , where  $|g_3\rangle = (|0000\rangle + |1110\rangle)/\sqrt{2}$ .

<sup>4</sup>Recently, the three-tangle of the GHZ-symmetric states [22] has been computed analytically [23].

In Ref. [31] another multipartite monogamy relation is derived:

$$\begin{aligned} \mathcal{C}_{q_1|q_2\cdots q_n}^2 &\geq \underbrace{\sum_{j=2}^n \mathcal{C}_{q_1|q_j}^2}_{\text{two-partite}} + \underbrace{\sum_{k>j=2}^n [\tau_{q_1|q_j|q_k}]^{\mu_3}}_{\text{three-partite}} + \cdots \\ &+ \underbrace{\sum_{\ell=2}^n [\tau_{q_1|q_2|\cdots|q_{\ell-1}|q_{\ell+1}|\cdots|q_n}]^{\mu_{n-1}}}_{(n-1)\text{-partite}}. \end{aligned} \quad (1.15)$$

In Eq. (1.15) the power factors  $\{\mu_m\}_{m=3}^{n-1}$  are included to regulate the weight assigned to the different  $m$ -partite contributions. If all power factors  $\mu_m$  go to infinity, Eq. (1.15) reduces to Eq. (1.13). In particular, the authors in Ref. [31] have conjectured  $\mu_3 = 3/2$ . Thus, in the four-qubit system one can construct another possible candidate of the tangle-based entanglement measure

$$t_2 = \frac{\sigma_A + \sigma_B + \sigma_C + \sigma_D}{4}, \quad (1.16)$$

where  $\sigma_A = \mathcal{C}_{A|(BCD)}^2 - (\mathcal{C}_{A|B}^2 + \mathcal{C}_{A|C}^2 + \mathcal{C}_{A|D}^2) - ([\tau_{A|B|C}]^\mu + [\tau_{A|B|D}]^\mu + [\tau_{A|C|D}]^\mu)$ , and others are obtained by changing the focusing qubit. One can show easily  $t_2(g_3) = 0$ . Thus, the measure  $t_2$  cannot be excluded as a true four-way entanglement measure.

In Refs. [32,33] two different negativity-based monogamy relations have been examined. From these relations one can construct the following candidates of the four-party entanglement measures:

$$n_1 = \frac{u_A + u_B + u_C + u_D}{4}, \quad (1.17)$$

where  $u_A = \mathcal{N}_{A|(BCD)} - (\mathcal{N}_{A|B} + \mathcal{N}_{A|C} + \mathcal{N}_{A|D}) - ([\mathcal{N}_{A||B|C}]^{v_1} + [\mathcal{N}_{A||B|D}]^{v_1} + [\mathcal{N}_{A||C|D}]^{v_1})$  with  $\mathcal{N}_{I||J|K} \equiv \mathcal{N}_{I|(JK)} - \mathcal{N}_{I|J} - \mathcal{N}_{I|K}$  and

$$n_2 = \frac{v_A + v_B + v_C + v_D}{4}, \quad (1.18)$$

where  $v_A = \mathcal{N}_{A|(BCD)}^2 - (\mathcal{N}_{A|B}^2 + \mathcal{N}_{A|C}^2 + \mathcal{N}_{A|D}^2) - ([\mathcal{N}_{A||B|C}]^{v_2} + [\mathcal{N}_{A||B|D}]^{v_2} + [\mathcal{N}_{A||C|D}]^{v_2})$  with  $\mathcal{N}_{I||J|K}^2 \equiv \mathcal{N}_{I|(JK)}^2 - \mathcal{N}_{I|J}^2 - \mathcal{N}_{I|K}^2$ . The negativity  $\mathcal{N}$  is defined as [34,35]

$$\mathcal{N}(\rho_{AB}) = \|\rho_{AB}^{T_A}\| - 1, \quad (1.19)$$

where  $\|X\| \equiv \text{tr}(\sqrt{XX^\dagger})$  and the superscript  $T_A$  means the partial transposition of the  $A$  qubit. Of course other quantities can be obtained by changing the focusing qubit.

The purpose of this paper is to test  $t_1$ ,  $t_2$ ,  $n_1$ , and  $n_2$  by computing them for the rank-2 mixture

$$\rho_4 = p|\text{GHZ}_4\rangle\langle\text{GHZ}_4| + (1-p)|W_4\rangle\langle W_4|, \quad (1.20)$$

where  $|\text{GHZ}_4\rangle$  is defined in Eq. (1.11) and  $|W_4\rangle = (\sigma_x \otimes \sigma_x \otimes \sigma_x \otimes \sigma_x)|\tilde{W}_4\rangle$ . In Sec. II we compute  $t_1$ ,  $t_2$ ,  $n_1$ , and  $n_2$  for the maximal entangled pure states (1.11) and  $|W_4\rangle$ . The results are summarized in Table II. It is shown that the negativity-based measures  $n_1$  and  $n_2$  become negative for  $|\Phi_3\rangle$ . In Sec. III we try to compute  $t_1$  and  $t_2$  for  $\rho_4$  by finding the optimal decompositions. For  $t_1$  it turns out that Eq. (1.20) itself is

TABLE II.  $t_1$ ,  $t_2$ ,  $n_1$ , and  $n_2$  of the maximally entangled and  $W_4$  states.

	$t_1$	$t_2$	$n_1$	$n_2$
$ \text{GHZ}_4\rangle$	1	1	1	1
$ \Phi_2\rangle$	1	1	$1 - 3(\frac{2}{3})^{v_1}$	$1 - 3(\frac{4}{9})^{v_2}$
$ \Phi_3\rangle$	1	1	-1	-1
$ W_4\rangle$	0	0	$\frac{3+\sqrt{3}-3\sqrt{2}}{2} - 3(\frac{3-2\sqrt{2}}{2})^{v_1}$	$\frac{3}{2}(\sqrt{2}-1) - 3(\frac{4\sqrt{2}-5}{4})^{v_2}$

an optimal decomposition. However, we fail to compute  $t_2$  because analytic computation of the residual entanglement is extremely difficult. In Sec. IV we compute  $n_1$  and  $n_2$  for  $\rho_4$  in the range  $v_{1*} \leq v_1$  and  $v_{2*} \leq v_2$  by finding the optimal decompositions, where

$$\begin{aligned} v_{1*} &= \frac{\ln(\frac{3-3\sqrt{2}+\sqrt{3}}{6})}{\ln(\frac{3}{2}-\sqrt{2})} = 1.020\,53, \\ v_{2*} &= \frac{\ln(\frac{\sqrt{2}-1}{2})}{\ln(\sqrt{2}-\frac{5}{4})} = 0.871\,544. \end{aligned} \quad (1.21)$$

In this region  $n_1(W_4)$  and  $n_2(W_4)$  become non-negative. In Sec. V a brief conclusion is given. In the Appendix we try to explain why the computation of the residual entanglement is highly difficult.

## II. COMPUTATION OF $t_1$ , $t_2$ , $n_1$ , AND $n_2$ FOR FEW SPECIAL PURE STATES

In this section we compute  $t_1$ ,  $t_2$ ,  $n_1$ , and  $n_2$  for four-qubit maximally entangled states (1.11) and  $W$  state  $|W_4\rangle$ . The most special case is  $|\text{GHZ}_4\rangle$ , which gives  $t_1 = t_2 = n_1 = n_2 = 1$ . Since  $|W_4\rangle$  saturates the monogamy relations (1.13) and (1.15),  $t_1$  and  $t_2$  of  $|W_4\rangle$  are exactly zero. However,  $|W_4\rangle$  does not saturate the negativity-based monogamy relations. It is straightforward [33] to show that  $n_1$  and  $n_2$  of  $|W_4\rangle$  are

$$\begin{aligned} n_1(W_4) &= \frac{3+\sqrt{3}-3\sqrt{2}}{2} - 3\left(\frac{3-2\sqrt{2}}{2}\right)^{v_1}, \\ n_2(W_4) &= \frac{3}{2}(\sqrt{2}-1) - 3\left(\frac{4\sqrt{2}-5}{4}\right)^{v_2}. \end{aligned} \quad (2.1)$$

Thus, as we commented,  $n_1(W_4)$  and  $n_2(W_4)$  become non-negative when  $v_{1*} \leq v_1$  and  $v_{2*} \leq v_2$ .

For  $|\Phi_2\rangle$  it is easy to show that  $\mathcal{C}_{I|(JKL)} = 1$  and  $\mathcal{C}_{I|J} = 0$  for all  $\{I, J, K, L\} = \{A, B, C, D\}$ . The tripartite states derived from  $|\Phi_2\rangle\langle\Phi_2|$  by tracing over any one-party is given by

$$\rho_3^{(2)} = \frac{1}{2}|\psi_1\rangle\langle\psi_1| + \frac{1}{2}|W_3\rangle\langle W_3|, \quad (2.2)$$

where  $|\psi_1\rangle = (|000\rangle + \sqrt{2}|111\rangle)/\sqrt{3}$  and  $|W_3\rangle = (|001\rangle + |010\rangle + |100\rangle)/\sqrt{3}$ . In order to compute the residual entanglement of  $\rho_3^{(2)}$  let us consider the quantum state  $p|g\text{GHZ}\rangle\langle g\text{GHZ}| + (1-p)|gW\rangle\langle gW|$ , where  $|g\text{GHZ}\rangle = a|000\rangle + b|111\rangle$  and  $|gW\rangle = c|001\rangle + d|010\rangle + f|100\rangle$ . As the second reference of Ref. [21] has shown, the residual entanglement of this state is exactly zero when  $p \leq p_0 \equiv s^{2/3}/(1+s^{2/3})$  where  $s = 4cdf/(a^2b)$ . Since, for our case,

$p_0 = 2/3$  is larger than  $1/2$ , the residual entanglement of  $\rho_3^{(2)}$  is zero. Thus,  $t_1$  and  $t_2$  of  $|\Phi_2\rangle$  are

$$t_1(\Phi_2) = t_2(\Phi_2) = 1. \quad (2.3)$$

Various negativities of  $|\Phi_2\rangle$  can be directly computed and the final expressions are

$$\mathcal{N}_{I|(JKL)} = 1, \quad \mathcal{N}_{I|(JK)} = \frac{2}{3}, \quad \mathcal{N}_{I|J} = 0 \quad (2.4)$$

for all  $\{I, J, K, L\} = \{A, B, C, D\}$ . Thus, it is easy to show

$$n_1(\Phi_2) = 1 - 3\left(\frac{2}{3}\right)^{v_1}, \quad n_2(\Phi_2) = 1 - 3\left(\frac{4}{9}\right)^{v_2}. \quad (2.5)$$

For  $|\Phi_3\rangle$  one can show  $\mathcal{C}_{I|(JKL)} = 1$  and  $\mathcal{C}_{I|J} = 0$  for all  $\{I, J, K, L\}$ . The tripartite states derived from  $|\Phi_3\rangle\langle\Phi_3|$  are

$$\begin{aligned} \rho_{ACD}^{(3)} &= \rho_{BCD}^{(3)} = \frac{1}{2}|\phi_1\rangle\langle\phi_1| + \frac{1}{2}|\phi_2\rangle\langle\phi_2|, \\ \rho_{ABC}^{(3)} &= \rho_{ABD}^{(3)} = \frac{1}{2}|g_1\rangle\langle g_1| + \frac{1}{2}|g_2\rangle\langle g_2|, \end{aligned} \quad (2.6)$$

where

$$\begin{aligned} |\phi_1\rangle &= \frac{1}{\sqrt{2}}(|100\rangle + |111\rangle), \quad |\phi_2\rangle = \frac{1}{\sqrt{2}}(|001\rangle + |010\rangle), \\ |g_1\rangle &= \frac{1}{\sqrt{2}}(|000\rangle + |111\rangle), \quad |g_2\rangle = \frac{1}{\sqrt{2}}(|001\rangle + |110\rangle). \end{aligned} \quad (2.7)$$

It is easy to show that the residual entanglements of  $\rho_{ACD}^{(3)}$  and  $\rho_{BCD}^{(3)}$  are zero because  $|\phi_1\rangle$  and  $|\phi_2\rangle$  are biseparable. In order to compute the residual entanglement of  $\rho_{ABC}^{(3)}$  and  $\rho_{ABD}^{(3)}$  let us consider the quantum state  $p|g_1\rangle\langle g_1| + (1-p)|g_2\rangle\langle g_2|$ . As the last reference of Ref. [21] has shown, the residual entanglement of this state is  $(2p-1)^2$ . Thus, the residual entanglements of  $\rho_{ABC}^{(3)}$  and  $\rho_{ABD}^{(3)}$  are also zero, all of which yields

$$t_1(\Phi_3) = t_2(\Phi_3) = 1. \quad (2.8)$$

Various negativities of  $|\Phi_3\rangle$  can be computed directly and the final expressions are

$$\mathcal{N}_{I|(JKL)} = 1, \quad \mathcal{N}_{I|J} = 0 \quad (2.9)$$

for all  $\{I, J, K, L\} = \{A, B, C, D\}$  and

$$\begin{aligned} \mathcal{N}_{A|(CD)} &= \mathcal{N}_{B|(CD)} = \mathcal{N}_{C|(AB)} = \mathcal{N}_{D|(AB)} = 0, \\ \mathcal{N}_{A|(BC)} &= \mathcal{N}_{A|(BD)} = \mathcal{N}_{B|(AC)} = \mathcal{N}_{B|(AD)} = \mathcal{N}_{C|(AD)} \\ &= \mathcal{N}_{C|(BD)} = \mathcal{N}_{D|(AC)} = \mathcal{N}_{D|(BC)} = 1, \end{aligned} \quad (2.10)$$

all of which yields

$$n_1(\Phi_3) = n_2(\Phi_3) = -1. \quad (2.11)$$

All results are summarized in Table II.

### III. TANGLE-BASED ENTANGLEMENT MEASURES FOR RANK-2 MIXTURE

In this section we try to compute  $t_1$  and  $t_2$  for the rank-2 mixture  $\rho_4$ . For computation of  $t_1$  and  $t_2$  we have to find an optimal decomposition. In order to find the optimal decompositions for  $t_1$  and  $t_2$  we define

$$|Z_4(p, \varphi)\rangle = \sqrt{p}|\text{GHZ}_4\rangle - e^{i\varphi}\sqrt{1-p}|W_4\rangle. \quad (3.1)$$

Then, one can show that all reduced bipartite states from  $|Z_4(p, \varphi)\rangle\langle Z_4(p, \varphi)|$  are equal to

$$\rho_{IJ} = \frac{1}{2} \begin{pmatrix} 1 & -\sqrt{\frac{p(1-p)}{2}}e^{-i\varphi} & -\sqrt{\frac{p(1-p)}{2}}e^{-i\varphi} & 0 \\ -\sqrt{\frac{p(1-p)}{2}}e^{i\varphi} & \frac{1-p}{2} & \frac{1-p}{2} & 0 \\ -\sqrt{\frac{p(1-p)}{2}}e^{i\varphi} & \frac{1-p}{2} & \frac{1-p}{2} & 0 \\ 0 & 0 & 0 & p \end{pmatrix} \quad (I, J \in \{A, B, C, D\}) \quad (3.2)$$

in the computational basis. In Eq. (3.2) the parties  $I$  and  $J$  can be chosen as any two different parties from  $\{A, B, C, D\}$ . Although  $\rho_{IJ}$  is a rank-3 mixture, one can compute its concurrence analytically by following Wootters procedure:

$$\mathcal{C}_{I|J} = \sqrt{\Lambda} - \sqrt{\Lambda_+} - \sqrt{\Lambda_-}, \quad (3.3)$$

where

$$\begin{aligned} \Lambda &= \frac{1}{12}[(1+p^2) + 2(\alpha^2 + \beta^2)^{1/6} \cos \theta], \\ \Lambda_{\pm} &= \frac{1}{12} \left[ (1+p^2) - 2(\alpha^2 + \beta^2)^{1/6} \cos \left( \frac{\pi}{3} \pm \theta \right) \right], \end{aligned} \quad (3.4)$$

and

$$\begin{aligned} \alpha &= 1 - 9p + 39p^2 - 90p^3 + \frac{231}{2}p^4 - 81p^5 + \frac{47}{2}p^6, \\ \beta &= \frac{3p^2(1-p)}{2} \\ &\times \sqrt{3p(4 - 28p + 96p^2 - 147p^3 + 110p^4 - 31p^5)}, \\ \theta &= \frac{1}{3} \tan^{-1} \left( \frac{\beta}{\alpha} \right). \end{aligned} \quad (3.5)$$

It is interesting to note that  $\mathcal{C}_{I|J} = 0$  at  $p = 1/3$ . Furthermore, it is worthwhile noting that  $\mathcal{C}_{I|J}$  is independent of the phase factor  $\varphi$ . On the contrary, the corresponding concurrence  $\mathcal{C}_{I|J}^{(3)}$  derived from the three-qubit state  $|Z_3(p, \varphi)\rangle = \sqrt{p}|\text{GHZ}_3\rangle - e^{i\varphi}\sqrt{1-p}|W_3\rangle$  is explicitly dependent on  $\varphi$ . The  $p$  dependencies of  $\mathcal{C}_{I|J}$  and  $\mathcal{C}_{I|J}^{(3)}$  are plotted in Fig. 1. The  $\varphi$  dependence of  $\mathcal{C}_{I|J}^{(3)}$  makes the three-qubit rank-2 mixture  $\rho_3 = p|\text{GHZ}_3\rangle\langle\text{GHZ}_3| + (1-p)|W_3\rangle\langle W_3|$  have the nontrivial residual entanglement [21]. As we will show shortly, the  $\varphi$  independence of  $\mathcal{C}_{I|J}$  makes  $t_1$  of  $\rho_4$  become trivial.

The single qubit states derived from  $|Z_4(p, \varphi)\rangle\langle Z_4(p, \varphi)|$  are all equal to

$$\rho_J = \begin{pmatrix} \frac{3-p}{4} & -\frac{1}{2}\sqrt{\frac{p(1-p)}{2}}e^{-i\varphi} \\ -\frac{1}{2}\sqrt{\frac{p(1-p)}{2}}e^{i\varphi} & \frac{1+p}{4} \end{pmatrix} \quad (J \in \{A, B, C, D\}) \quad (3.6)$$

in the computational basis. Thus,  $\mathcal{C}_{I|(JKL)}^2$  for  $|Z_4(p, \varphi)\rangle$  is

$$\mathcal{C}_{I|(JKL)}^2 = 4 \det \rho_I = \frac{3+p^2}{4} \quad (3.7)$$

for all  $I, J, K, L$ . The corresponding result derived from  $|Z_3(p, \varphi)\rangle$  is  $(8 - 4p + 5p^2)/9$ .

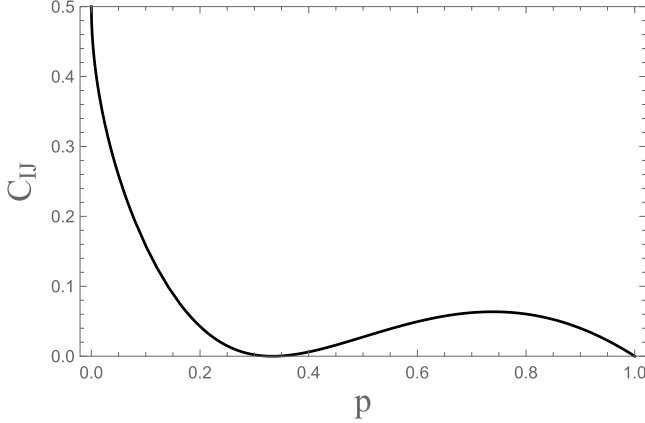


FIG. 1. The  $p$  dependence of (a)  $C_{IJ}$  and (b)  $C_{IJ}^{(3)}$ . As (a) shows,  $C_{IJ}$  is independent of the phase factor  $\varphi$  unlike  $C_{IJ}^{(3)}$ . This makes  $t_1(\rho_4)$  trivial.

Thus,  $t_1[Z_4(p, \varphi)]$  is independent of  $\varphi$  as

$$t_1[Z_4(p, \varphi)] = \frac{3 + p^2}{4} - 3C_{IJ}^2. \quad (3.8)$$

The corresponding residual entanglement  $\tau[Z_3(p, \varphi)]$  for  $|Z_3(p, \varphi)\rangle$  is dependent on  $\varphi$  due to  $C_{IJ}^{(3)}$ . The  $p$  dependence of  $t_1[Z_4(p, \varphi)]$  and  $\tau[Z_3(p, \varphi)]$  is plotted in Figs. 2(a) and 2(b), respectively.

Before we calculate  $t_1(\rho_4)$ , it seems to be helpful to review briefly how to compute  $\tau(\rho_3)$  for  $\rho_3 = p|GHZ_3\rangle\langle GHZ_3| + (1-p)|W_3\rangle\langle W_3|$ . As Fig. 2(b) shows, when  $\varphi = 0$   $\tau[Z_3(p, \varphi)]$  has nontrivial zero at  $p = p_0$  with  $p_0 \sim 0.627$ . Furthermore,  $\tau[Z_3(p, \varphi = 0)]$  is not convex in the regions  $0 \leq p \leq p_0$  and  $p_1 \leq p \leq 1$  with  $p_1 \sim 0.826$ . Since  $\tau[Z_3(p, \varphi)]$  depends on  $\varphi$  through only  $\cos 3\varphi$ ,  $\tau[Z_3(p_0, \varphi)] = 0$  for  $\varphi = 0, 2\pi/3, 4\pi/3$ . Thus, at the small concave region it is possible to convexify the residual entanglement by making use of  $\{|W_3\rangle, |Z_3(p, \frac{2\pi}{3}j)\rangle\}$  ( $j = 0, 1, 2$ ). At the large concave region it is also possible to convexify it by making use of  $\{|GHZ_3\rangle, |Z_3(p, \frac{2\pi}{3}j)\rangle\}$  ( $j = 0, 1, 2$ ).

Now, let us return to the four-qubit case. As Fig. 2(a) shows,  $t_1[Z_4(p, \varphi)]$  is not convex at  $0 \leq p \leq p_0$  and  $p_1 \leq p \leq 1$  with  $p_0 \sim 0.279$  and  $p_1 \sim 0.936$ . As for the three-qubit case, it is possible to convexify the entanglement by making use of  $\{|GHZ_4\rangle, |Z_4(p, 0)\rangle, |Z_4(p, \pi)\rangle\}$  in the large  $p$  region.

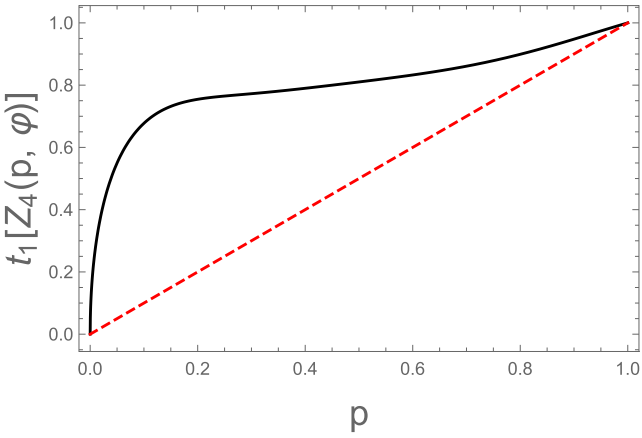
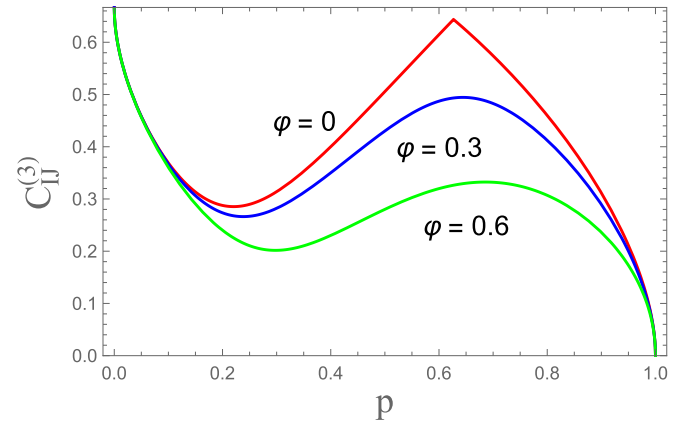


FIG. 2. The  $p$  dependence of (a)  $t_1[Z_4(p, \varphi)]$  and (b)  $\tau[Z_3(p, \varphi)]$ . Contrary to  $\tau[Z_3(p, \varphi)]$ ,  $t_1[Z_4(p, \varphi)]$  is independent of the phase factor  $\varphi$ .



However, it is impossible to convexify it in the small  $p$  region because  $t_1[Z_4(p_0, 0)] \neq 0$ . The only way to obtain the convex result in the entire range of  $p$  is

$$t_1(\rho_4) = p. \quad (3.9)$$

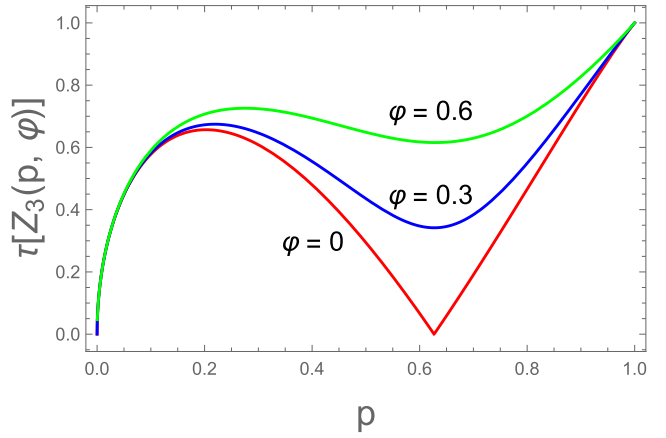
As Fig. 2(a) shows obviously as a dashed line, this is a convex hull of  $t_1[Z_4(p, \varphi)]$ . Thus, the optimal decomposition for  $t_1$  is nothing but the spectral decomposition (1.20) itself.

In order to compute  $t_2(\rho_4)$  we should compute the residual entanglement for the three-qubit states reduced from  $|Z_4(p, \varphi)\rangle$ . One can show that all tripartite states derived by tracing over a single qubit are equal to

$$\rho_{IJK} = \lambda|\psi_+\rangle\langle\psi_+| + (1-\lambda)|\psi_-\rangle\langle\psi_-| \quad (I, J, K \in \{A, B, C, D\}), \quad (3.10)$$

where

$$\begin{aligned} \lambda &= \frac{2 + \sqrt{1 - p^2}}{4}, \\ |\psi_\pm\rangle &= \frac{1}{N_\pm} [\mu_\pm|000\rangle - e^{-i\varphi}|111\rangle \\ &\quad - v_\pm e^{i\varphi}(|001\rangle + |010\rangle + |100\rangle)] \end{aligned} \quad (3.11)$$



with

$$\begin{aligned} N_{\pm}^2 &= \frac{(1+p)(3-p) \pm (3+p)\sqrt{1-p^2}}{2p^2}, \\ \mu_{\pm} &= \frac{2(1-p) \pm \sqrt{1-p^2}}{\sqrt{2p(1-p)}}, \\ v_{\pm} &= \frac{(3+p)(1-p) \pm (3-p)\sqrt{1-p^2}}{2p(2 \pm \sqrt{1-p^2})}. \end{aligned} \quad (3.12)$$

The residual entanglement for  $|\psi_{\pm}\rangle$  is

$$\tau(\psi_{\pm}) = \frac{4}{N_{\pm}^4} \sqrt{\mu_{\pm}^4 + 16v_{\pm}^6 + 8\mu_{\pm}^2 v_{\pm}^3 \cos 4\varphi}. \quad (3.13)$$

Thus, the spectral decomposition (3.10) indicates that the residual entanglement for  $\rho_{IJK}$  satisfies

$$\tau(\rho_{IJK}) \leq \lambda \tau(\psi_+) + (1-\lambda) \tau(\psi_-). \quad (3.14)$$

However, the analytic computation of the residual entanglement for  $\rho_{IJK}$  is highly difficult even though it is a rank-2 tensor. In the Appendix we try to describe why it is highly difficult. Therefore, we fail to compute  $t_2(\rho_4)$  analytically.

#### IV. NEGATIVITY-BASED ENTANGLEMENT MEASURES FOR RANK-2 MIXTURE

In this section we try to compute  $n_1$  and  $n_2$  for  $\rho_4$ . We consider only the regions  $v_{1*} \leq v_1 \leq \infty$  and  $v_{2*} \leq v_2 \leq \infty$ , where  $v_{1*}$  and  $v_{2*}$  are given in Eq. (1.21). When  $v_1 = v_{1*}$  and  $v_2 = v_{2*}$ ,  $n_1(W_4) = n_2(W_4) = 0$  exactly. When  $v_1 = v_2 = \infty$ ,  $n_1$  and  $n_2$  for  $|W_4\rangle$  become

$$\begin{aligned} n_1(W_4) &= \frac{3 + \sqrt{3} - 3\sqrt{2}}{2} = 0.244705, \\ n_2(W_4) &= \frac{3}{2}(\sqrt{2} - 1) = 0.62132. \end{aligned} \quad (4.1)$$

Of course,  $n_1$  and  $n_2$  for  $|\text{GHZ}_4\rangle$  are unity regardless of  $v_1$  and  $v_2$ .

In order to find the optimal decompositions for  $n_1(\rho_4)$  and  $n_2(\rho_4)$  we reconsider  $|Z_4(p, \varphi)\rangle$  defined in Eq. (3.1). By direct calculation one can show straightforwardly

$$N_{I|JKL} = \frac{1}{2}\sqrt{3 + p^2}, \quad (4.2)$$

where  $I, J, K, L$  are any one of  $\{A, B, C, D\}$ .

Using Eq. (3.2) one can also show that any bipartite negativity  $N_{I|J}$  for  $|Z_4(p, \varphi)\rangle$  is

$$N_{I|J} = \sqrt{\lambda} + \sqrt{\lambda_+} + \sqrt{\lambda_-} - \frac{3+p}{4}, \quad (4.3)$$

where

$$\begin{aligned} \lambda &= \frac{1}{48}[(7+2p-p^2) + 4r_0 \cos \theta_0], \\ \lambda_{\pm} &= \frac{1}{48} \left[ (7+2p-p^2) - 4r_0 \cos \left( \frac{\pi}{3} \pm \theta_0 \right) \right] \end{aligned} \quad (4.4)$$

with

$$r_0 = (\alpha_0^2 + \beta_0^2)^{1/6}, \quad \theta_0 = \frac{1}{3} \tan^{-1} \left( \frac{\beta_0}{\alpha_0} \right),$$

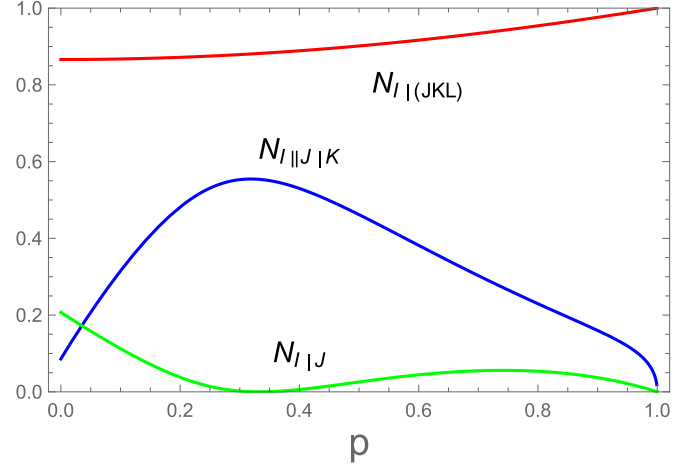


FIG. 3. The  $p$  dependence of  $N_{I|JKL}$ ,  $N_{I||J|K}$ , and  $N_{I|J}$  for  $|Z(p, \varphi)\rangle$ . It is shown that all negativities are independent of the phase factor  $\varphi$ .

$$\begin{aligned} \alpha_0 &= 17 + 147p - 153p^2 - 428p^3 \\ &\quad + 729p^4 - 447p^5 + 127p^6, \\ \beta_0 &= 3\sqrt{3}(1 - p + 5p^2 - 7p^3 + 2p^4) \\ &\quad \times \sqrt{2 + 4p - 71p^2 + 214p^3 - 129p^4}. \end{aligned} \quad (4.5)$$

Like the concurrence discussed in the previous section,  $N_{I|J}$  becomes zero when  $p = 1/3$  and  $p = 1$ .

Finally, we compute  $N_{I||JK}$  for all  $I, J, K \in \{A, B, C, D\}$ . Using Eq. (3.10) one can compute the nonzero eigenvalues of  $(\rho_{IJK}^{T_I})(\rho_{IJK}^{T_I})^\dagger$ . One of them is  $p^2/4$  and the remaining five nonzero eigenvalues can be obtained by solving the quintic equation. Thus, it is possible to compute  $N_{I||JK}$  numerically. After obtaining  $N_{I||JK}$ , one can compute  $N_{I||J|K}$  and  $N_{I||J|K}^2$  by making use of  $N_{I||J|K} = N_{I||JK} - (N_{I|J} + N_{I|K})$  and  $N_{I||J|K}^2 = N_{I||JK}^2 - (N_{I|J}^2 + N_{I|K}^2)$ . It is worthwhile noting that all negativities are independent of the phase angle  $\varphi$ . Thus,  $n_1(\rho_4)$  and  $n_2(\rho_4)$  are independent of  $\varphi$ . In Fig. 3 we plot the  $p$  dependence of  $N_{I|JKL}$ ,  $N_{I||J|K}$ , and  $N_{I|J}$ .

In Fig. 4(a) we plot the  $p$  dependence of  $n_1[Z(p, \varphi)]$  for  $|Z_4(p, \varphi)\rangle$  when  $v_1 = v_{1*}$  (red dashed line) and  $v_1 = \infty$  (blue dotted line). When  $v_1 = v_{1*}$ ,  $n_1[Z(p, \varphi)]$  becomes negative at  $0 < p < p_0$ , where  $p_0 = 0.749596$ . Since, however,  $n_1(W_4) = 0$  at  $v_1 = v_{1*}$ , one can choose the optimal decomposition for  $\rho_4(p)$  in this region as

$$\begin{aligned} \rho_4(p) &= \frac{p}{2p_0} [|Z_4(p_0, 0)\rangle\langle Z_4(p_0, 0)| + |Z_4(p_0, \pi)\rangle\langle Z_4(p_0, \pi)|] \\ &\quad + \left( 1 - \frac{p}{p_0} \right) |W_4\rangle\langle W_4|, \end{aligned} \quad (4.6)$$

which gives  $n_1(\rho_4) = 0$  at  $0 \leq p \leq p_0$ . At  $p_0 \leq p \leq 1$  the optimal decomposition for  $\rho_4(p)$  is

$$\rho_4(p) = \frac{1}{2} [|Z_4(p, 0)\rangle\langle Z_4(p, 0)| + |Z_4(p, \pi)\rangle\langle Z_4(p, \pi)|], \quad (4.7)$$

which gives  $n_1(\rho_4) = n_1[Z(p, \varphi)]$  at  $p_0 \leq p \leq 1$ . Since  $n_1[Z(p, \varphi)]$  is convex in this region, we do not need to convexify it. Thus, our result for  $n_1(\rho_4)$  at  $v_1 = v_{1*}$  can be

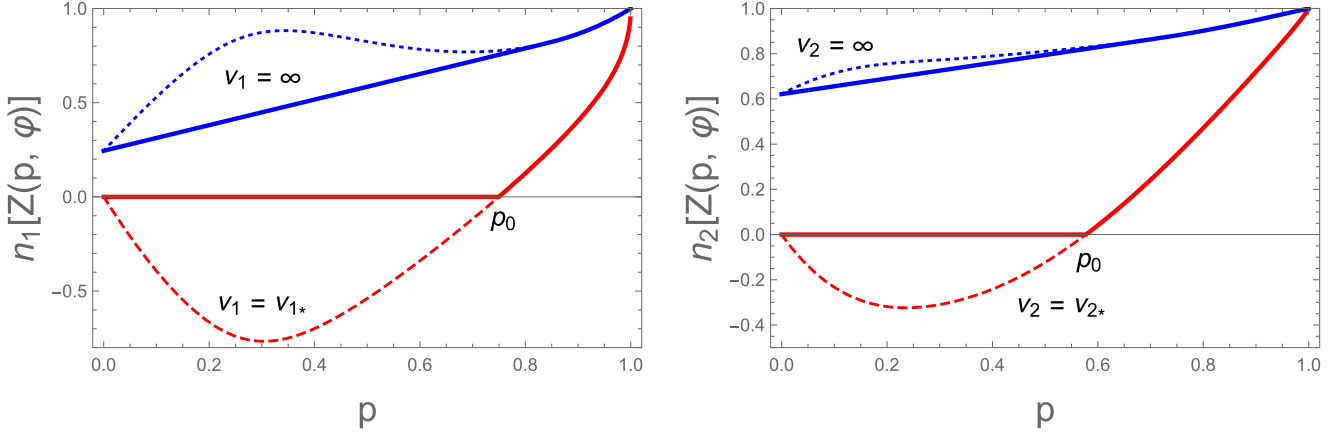


FIG. 4. The  $p$  dependence of (a)  $n_1[Z(p,\varphi)]$  (dashed and dotted) and  $n_1(\rho_4)$  (solid) at  $v_1 = v_{1*}$  [red (lower) solid] and  $v_1 = \infty$  [blue (upper) solid], and (b)  $n_2[Z(p,\varphi)]$  (dashed and dotted) and  $n_2(\rho_4)$  (solid) at  $v_2 = v_{2*}$  [red (lower) solid] and  $v_2 = \infty$  [blue (upper) solid].

expressed as

$$n_1(\rho_4) = \begin{cases} 0, & 0 \leq p \leq p_0 = 0.749596 \\ n_1[Z(p,0)], & p_0 \leq p \leq 1. \end{cases} \quad (4.8)$$

This is plotted in Fig. 4(a) as a red (lower) solid line.

When  $v_1 = \infty$ ,  $n_1[Z(p,\varphi)]$  is not convex at the region  $0 \leq p \leq p_*$  with  $p_* \approx 0.475$ . Thus, we have to convexify it at the region  $0 \leq p \leq p_1$  with  $p_1 > p_*$ . We will fix  $p_1$  later. At the region  $0 \leq p \leq p_1$  we choose an optimal decomposition for  $\rho_4(p)$  as

$$\rho_4(p) = \frac{p_1 - p}{p_1} |W_4\rangle\langle W_4| + \frac{p}{2p_1} [|Z_4(p_1,0)\rangle\langle Z_4(p_1,0)| + |Z_4(p_1,\pi)\rangle\langle Z_4(p_1,\pi)|]. \quad (4.9)$$

From Eq. (4.9)  $n_1(\rho_4)$  becomes  $g(p)$ , where

$$g(p) = \frac{3 + \sqrt{3} - 3\sqrt{2}}{2} \frac{p_1 - p}{p_1} + \frac{p}{p_1} n_1[Z(p_1,0)]. \quad (4.10)$$

Then,  $p_1$  is determined by  $\partial g(p, p_1)/\partial p_1 = 0$ , which gives  $p_1 \approx 0.84$ . Thus, finally  $n_1(\rho_4)$  at  $v_1 = \infty$  is given by

$$n_1(\rho_4) = \begin{cases} g(p), & 0 \leq p \leq p_1 \approx 0.84 \\ n_1[Z(p,0)], & p_1 \leq p \leq 1. \end{cases} \quad (4.11)$$

This is plotted in Fig. 4(a) as a blue (upper) solid line.

In Fig. 4(b) we plot the  $p$  dependence of  $n_2[Z(p,\varphi)]$  for  $|Z_4(p,\varphi)\rangle$  when  $v_2 = v_{2*}$  (red dashed line) and  $v_2 = \infty$  (blue dotted line). When  $v_2 = v_{2*}$ ,  $n_2[Z(p,\varphi)]$  becomes negative at the region  $0 \leq p \leq p_0$ , where  $p_0 = 0.57731$ . Following a similar procedure in the case of  $v_1 = v_{1*}$  one can derive  $n_2(\rho_4)$  as

$$n_2(\rho_4) = \begin{cases} 0, & 0 \leq p \leq p_0 = 0.57731 \\ n_2[Z(p,0)], & p_0 \leq p \leq 1. \end{cases} \quad (4.12)$$

This is plotted in Fig. 4(b) as a red (lower) solid line.

For the  $v_2 = \infty$  case  $n_2[Z(p,\varphi)]$  is not convex at  $0 \leq p \leq p_{1*}$  and  $p_{2*} \leq p \leq 1$ , where  $p_{1*} \approx 0.25$  and  $p_{2*} \approx 0.95$ . Thus, we have to convexify  $n_2(\rho_4)$  in the small- $p$  and large- $p$  regions. First we choose a small- $p$  region  $0 \leq p \leq p_1$  with  $p_{1*} \leq p_1 \leq p_{2*}$ . The parameter  $p_1$  will be fixed later. In this

region we choose the optimal decomposition as Eq. (4.9). Then,  $n_2(\rho_4)$  becomes  $f_I(p)$ , where

$$f_I(p) = \frac{3}{2}(\sqrt{2} - 1) \frac{p_1 - p}{p_1} + \frac{p}{p_1} n_2[Z(p_1,0)]. \quad (4.13)$$

Then,  $p_1$  is fixed by  $\partial f_I(p, p_1)/\partial p_1 = 0$ , which gives  $p_1 \approx 0.72$ . Next, we consider the large- $p$  region  $p_2 \leq p \leq 1$  with  $p_1 \leq p_2 \leq p_{2*}$ . In this region the optimal decomposition can be chosen as

$$\begin{aligned} \rho_4(p) = & \frac{p - p_2}{1 - p_2} |\text{GHZ}_4\rangle\langle \text{GHZ}_4| \\ & + \frac{1 - p}{2(1 - p_2)} [|Z_4(p_2,0)\rangle\langle Z_4(p_2,0)| \\ & + |Z_4(p_2,\pi)\rangle\langle Z_4(p_2,\pi)|]. \end{aligned} \quad (4.14)$$

Thus,  $n_2(\rho_4)$  becomes  $f_{II}(p)$  in this region, where

$$f_{II}(p) = \frac{p - p_2}{1 - p_2} + \frac{1 - p}{1 - p_2} n_2[Z(p_2,0)]. \quad (4.15)$$

The parameter  $p_2$  is fixed by  $\partial f_{II}(p, p_2)/\partial p_2 = 0$ , which gives  $p_2 \approx 0.92$ . Thus, the final expression  $n_2(\rho_4)$  for the  $v_2 = \infty$  case can be written in a form

$$n_2(\rho_4) = \begin{cases} f_I(p), & 0 \leq p \leq p_1 \approx 0.72 \\ n_2[Z(p,0)], & p_1 \leq p \leq p_2 \approx 0.92 \\ f_{II}(p), & p_2 \leq p \leq 1. \end{cases} \quad (4.16)$$

This is plotted as a blue (upper) solid line in Fig. 4(b).

## V. CONCLUSIONS

In this paper we compute the monogamy-motivated four-party measures  $n_1$ ,  $n_2$ ,  $t_1$ , and  $t_2$  for the rank-2 mixtures  $\rho_4$  given in Eq. (1.20). It turns out that  $t_1(\rho_4)$  is trivial and the corresponding optimal decomposition is equal to the spectral decomposition. Probably, this triviality is a sign of the fact that monogamy relation (1.13) is not sufficiently tight, which means that  $t_1$  is not a true four-way entanglement measure. We fail to compute  $t_2(\rho_4)$  analytically because it is highly difficult to compute the residual entanglement for the rank-2 state (3.10), which is a tripartite state reduced

from  $|Z_4(p,\varphi)\rangle\langle Z_4(p,\varphi)|$ . This difficulty is discussed in the Appendix.

We also compute  $n_1$  and  $n_2$  for  $\rho_4$  when  $v_j = v_{j*}$  ( $j = 1, 2$ ) or  $\infty$ . When  $v_1 = v_{1*}$  the final expression of  $n_1(\rho_4)$  is Eq. (4.8) and the corresponding optimal decompositions are (4.6) in  $0 \leq p \leq p_0$  and (4.7) in  $p_0 \leq p \leq 1$ , where  $p_0 \sim 0.749\,596$ . When  $v_1 = \infty$ , the final expression of  $n_1(\rho_4)$  is Eq. (4.11) and the corresponding optimal decompositions are (4.9) in  $0 \leq p \leq p_1$  and (4.7) in  $p_1 \leq p \leq 1$ , where  $p_1 \sim 0.84$ . When  $v_2 = v_{2*}$  and  $v_2 = \infty$ , the final expressions of  $n_2(\rho_4)$  are Eq. (4.12) and Eq. (4.16), respectively, and the corresponding optimal decompositions can be found in the previous section. As Table II shows,  $n_1$  and  $n_2$  are not always non-negative for all four-qubit pure states. This means that the corresponding negativity-based monogamy relations discussed in Refs. [32,33] do not always hold regardless of the power factor  $v_1$  and  $v_2$ .

It is most important for us to check whether or not  $t_2$  is a true four-way entanglement measure when the power factor  $\mu_3$  is chosen appropriately. As we mentioned, we fail to check this fact in this paper due to the difficulty in the analytic computation of the residual entanglement of the tripartite reduced state (3.10). We hope to discuss this issue again in the near future.

## APPENDIX

In this Appendix we try to explain why the analytic computation of the residual entanglement for  $\rho_{IJK}$  in Eq. (3.10) is difficult by introducing a simpler rank-2 quantum state

$$\Pi = p|\psi_1\rangle\langle\psi_1| + (1-p)|\psi_2\rangle\langle\psi_2|, \quad (\text{A1})$$

where

$$|\psi_1\rangle = \frac{1}{\sqrt{2}}(|\text{GHZ}_3\rangle + |W_3\rangle),$$

$$\tau_3(p,\varphi) = 2\sqrt{(1 - 2\sqrt{p(1-p)}\cos\varphi)[f_0(p) + f_1(p)\cos\varphi + f_2(p)\cos 2\varphi + f_3(p)\cos 3\varphi]}, \quad (\text{A8})$$

where

$$\begin{aligned} f_0(p) &= \frac{155}{1728}(1 + 6p - 6p^2) + \frac{2p - 1}{6\sqrt{6}}(1 - 10p + 10p^2), \\ f_1(p) &= \frac{101}{288}\sqrt{p(1-p)}(1 + p - p^2), \\ f_2(p) &= 6p(1-p)\left(\frac{155}{1728} + \frac{2p - 1}{6\sqrt{6}}\right), \\ f_3(p) &= \frac{101}{864}\sqrt{p^3(1-p)^3}. \end{aligned} \quad (\text{A9})$$

From Eq. (A6) one can show that  $\tau_3(p,\varphi)$  becomes zero at particular  $p$  and  $\varphi$ . These nontrivial zeros are summarized in Table III. From Eq. (A8) one can show that  $\tau_3(p,\varphi)$  has a

TABLE III. Nontrivial zeros of  $\tau_3(p,\varphi)$  with  $\varphi_0 = 1.276\,72$ .

$\varphi$	$\pi$	0	$\pi \pm \varphi_0$
$p$	$p_1 = 0.0163588$	$p_2 = 0.5$	$p_3 = 0.741\,82$

$$|\psi_2\rangle = \frac{1}{\sqrt{2}}(|\text{GHZ}_3\rangle - |W_3\rangle). \quad (\text{A2})$$

In spite of its simpleness  $\Pi$  has the same structure with  $\rho_{IJK}$ . The residual entanglements of  $|\psi_1\rangle$  and  $|\psi_2\rangle$  are

$$\begin{aligned} \tau_3(\psi_1) &= \frac{8\sqrt{6} + 9}{36} = 0.794\,331, \\ \tau_3(\psi_2) &= \frac{8\sqrt{6} - 9}{36} = 0.294\,331. \end{aligned} \quad (\text{A3})$$

Thus,  $\tau_3(\Pi)$  has an upper bound as

$$\tau_3(\Pi) \leq \tau_3^{\max} = \frac{p}{2} + \frac{8\sqrt{6} - 9}{36}. \quad (\text{A4})$$

In order to compute  $\tau_3(\Pi)$  we define the superposed state

$$|Z(p,\varphi)\rangle = \sqrt{p}|\psi_1\rangle - e^{i\varphi}\sqrt{1-p}|\psi_2\rangle. \quad (\text{A5})$$

The residual entanglement  $\tau_3(p,\varphi)$  of  $|Z(p,\varphi)\rangle$  can be written as

$$\tau_3(p,\varphi) = 4p^2 \left| \frac{1-z}{2} \right| \left| \frac{1}{8}(1-z)^3 + \frac{2}{3\sqrt{6}}(1+z)^3 \right|, \quad (\text{A6})$$

where

$$z = e^{i\varphi} \sqrt{\frac{1-p}{p}}. \quad (\text{A7})$$

Another useful expression of  $\tau_3(p,\varphi)$  is

symmetry

$$\tau_3(p,n\pi + \varphi_0) = \tau_3(p,n\pi - \varphi_0) \quad (\text{A10})$$

for all integer  $n$ .

In Fig. 5(a) we plot  $\tau_3(p,\varphi)$  at  $\varphi = 0, \pi \pm \varphi_0$ , and  $\pi$  with  $\varphi_0 = 1.276\,42$ . The nontrivial zeros  $p_1, p_2$ , and  $p_3$  given in Table III are plotted as black dots. In Fig. 5(b) we plot  $\tau_3(p,\varphi)$  for various  $\varphi$ . These curves have been referred to as the characteristic curves. The dashed line in both figures is the  $p$  dependence of  $\tau_3^{\max}$ . The red (lowest) solid line in Fig. 5(b) is a minimum of the characteristic curves. The authors of Ref. [36] have claimed that  $\tau_3(\Pi)$  is a convex hull of the minimum of the characteristic curves. If this is right, Fig. 5(b) seems to exhibit that  $\tau_3(\Pi)$  is zero at  $p_1 \leq p \leq p_3$ . However, it is very difficult to find the corresponding optimal decompositions. For example, let us consider the  $p = p_3$  case. Table III indicates that the corresponding optimal decomposition is  $(1/2)[|Z(p_3,\pi - \varphi_0)\rangle\langle Z(p_3,\pi - \varphi_0)| + |Z(p_3,\pi + \varphi_0)\rangle\langle Z(p_3,\pi + \varphi_0)|]$ . However, this is not equal to  $\Pi(p_3)$  because of the cross terms. Similar difficulties arise at  $p = p_1$  and  $p = p_2$ . So far, we do not know how to compute  $\tau_3(\Pi)$  analytically.

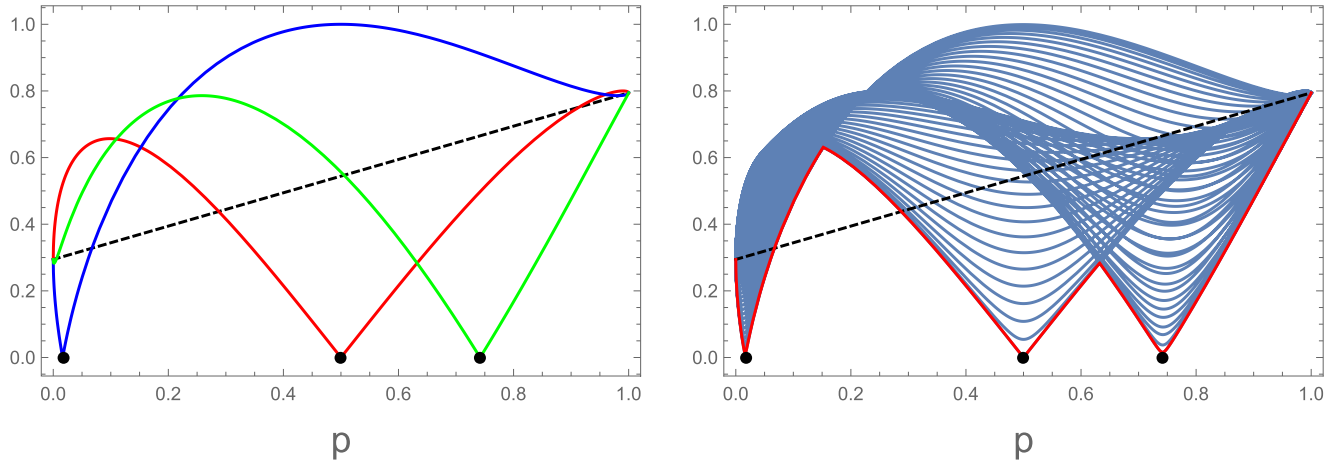


FIG. 5. (a) The  $p$  dependence of  $\tau_3(p,0)$ ,  $\tau_3(p,\pi)$ , and  $\tau_3(p,\pi \pm \varphi_0)$  with  $\varphi_0 = 1.27672$ . The dashed curve is a  $p$  dependence of  $\tau_3^{\max}$ . The nontrivial zeros given in Table III are plotted as black dots. (b) The  $p$  dependence of  $\tau_3(p,\varphi)$  with varying  $\varphi$  from 0 to  $\pi$  with a step 0.05. These curves have been referred to as the characteristic curves. The red (lowest) solid line is a minimum of the characteristic curves. This red curve seems to indicate that  $\tau_3(\Pi)$  is zero at  $p_1 \leq p \leq p_3$ . However, we cannot find the corresponding optimal decompositions.

- [1] A. Einstein, B. Podolsky, and N. Rosen, Can quantum-mechanical description of physical reality be considered complete? *Phys. Rev.* **47**, 777 (1935).
- [2] E. Schrödinger, Die gegenwärtige Situation in der Quantenmechanik, *Naturwissenschaften*, **23**, 807 (1935).
- [3] M. A. Nielsen and I. L. Chuang, *Quantum Computation and Quantum Information* (Cambridge University Press, Cambridge, England, 2000).
- [4] R. Horodecki, P. Horodecki, M. Horodecki, and K. Horodecki, Quantum entanglement, *Rev. Mod. Phys.* **81**, 865 (2009), and references therein.
- [5] C. H. Bennett, G. Brassard, C. Crepeau, R. Jozsa, A. Peres, and W. K. Wootters, Teleporting an Unknown Quantum State via Dual Classical and Einstein-Podolsky-Rosen Channels, *Phys. Rev. Lett.* **70**, 1895 (1993).
- [6] C. H. Bennett and S. J. Wiesner, Communication Via One- and Two-Particle Operators on Einstein-Podolsky-Rosen States, *Phys. Rev. Lett.* **69**, 2881 (1992).
- [7] V. Scarani, S. Lblisdir, N. Gisin, and A. Acin, Quantum cloning, *Rev. Mod. Phys.* **77**, 1225 (2005), and references therein.
- [8] A. K. Ekert, Quantum Cryptography Based on Bells Theorem, *Phys. Rev. Lett.* **67**, 661 (1991).
- [9] C. Kollmitzer and M. Pivk, *Applied Quantum Cryptography* (Springer, Heidelberg, 2010).
- [10] T. D. Ladd, F. Jelezko, R. Laflamme, Y. Nakamura, C. Monroe, and J. L. O'Brien, Quantum computers, *Nature (London)* **464**, 45 (2010).
- [11] G. Vidal, Efficient Classical Simulation of Slightly Entangled Quantum Computations, *Phys. Rev. Lett.* **91**, 147902 (2003).
- [12] C. H. Bennett, D. P. DiVincenzo, J. A. Smolin, and W. K. Wootters, Mixed-state entanglement and quantum error correction, *Phys. Rev. A* **54**, 3824 (1996).
- [13] V. Vedral, M. B. Plenio, M. A. Rippin, and P. L. Knight, Quantifying Entanglement, *Phys. Rev. Lett.* **78**, 2275 (1997).
- [14] V. Vedral and M. B. Plenio, Entanglement measures and purification procedures, *Phys. Rev. A* **57**, 1619 (1998).
- [15] A. Miranowicz and S. Ishizaka, Closed formula for the relative entropy of entanglement, *Phys. Rev. A* **78**, 032310 (2008); H. Kim, M.-R. Hwang, E. Jung, and D. K. Park, Difficulties in analytic computation for relative entropy of entanglement, *ibid.* **81**, 052325 (2010); D. K. Park, Relative entropy of entanglement for two-qubit state with  $z$ -directional Bloch vectors, *Int. J. Quantum Inf.* **08**, 869 (2010); S. Friedland and G. Gour, Closed formula for the relative entropy of entanglement in all dimensions, *J. Math. Phys.* **52**, 052201 (2011); M. W. Girard, G. Gour, and S. Friedland, On convex optimization problems in quantum information theory, *J. Phys. A: Math. Theor.* **47**, 505302 (2014); E. Jung and D. K. Park, REE From EOF, *Quantum Inf. Proc.* **14**, 531 (2015).
- [16] S. Hill and W. K. Wootters, Entanglement of a Pair of Quantum Bits, *Phys. Rev. Lett.* **78**, 5022 (1997); W. K. Wootters, Entanglement of Formation of an Arbitrary State of Two Qubits, *ibid.* **80**, 2245 (1998).
- [17] V. Coffman, J. Kundu, and W. K. Wootters, Distributed entanglement, *Phys. Rev. A* **61**, 052306 (2000).
- [18] W. Dür, G. Vidal, and J. I. Cirac, Three qubits can be entangled in two inequivalent ways, *Phys. Rev. A* **62**, 062314 (2000).
- [19] C. H. Bennett, S. Popescu, D. Rohrlich, J. A. Smolin, and A. V. Thapliyal, Exact and asymptotic measures of multipartite pure-state entanglement, *Phys. Rev. A* **63**, 012307 (2000).
- [20] A. Uhlmann, Fidelity and concurrence of conjugate states, *Phys. Rev. A* **62**, 032307 (2000).
- [21] R. Lohmayer, A. Osterloh, J. Siewert, and A. Uhlmann, Entangled Three-Qubit States without Concurrence and Three-Tangle, *Phys. Rev. Lett.* **97**, 260502 (2006); C. Eltschka, A. Osterloh, J. Siewert, and A. Uhlmann, Three-tangle for mixtures of generalized GHZ and generalized W states, *New J. Phys.* **10**, 043014 (2008); E. Jung, M. R. Hwang, D. K. Park, and

- J. W. Son, Three-tangle for rank-3 mixed states: Mixture of Greenberger-Horne-Zeilinger,  $W$  and flipped  $W$  states, *Phys. Rev. A* **79**, 024306 (2009); E. Jung, D. K. Park, and J. W. Son, Three-tangle does not properly quantify tripartite entanglement for Greenberger-Horne-Zeilinger-type state, *ibid.* **80**, 010301(R) (2009); E. Jung, M. R. Hwang, D. K. Park, and S. Tamaryan, Three-party entanglement in tripartite teleportation scheme through noisy channels, *Quantum Inf. Comput.* **10**, 0377 (2010).
- [22] C. Eltschka and J. Siewert, Entanglement of Three-Qubit Greenberger-Horne-Zeilinger-Symmetric States, *Phys. Rev. Lett.* **108**, 020502 (2012).
- [23] J. Siewert and C. Eltschka, Quantifying Tripartite Entanglement of Three-Qubit Generalized Werner States, *Phys. Rev. Lett.* **108**, 230502 (2012).
- [24] F. Verstraete, J. Dehaene, and D. De Moor, Normal forms and entanglement measures for multipartite quantum states, *Phys. Rev. A* **68**, 012103 (2003).
- [25] A. Osterloh and J. Siewert, Constructing  $N$ -qubit entanglement monotones from antilinear operators, *Phys. Rev. A* **72**, 012337 (2005); D. Ž. Doković and A. Osterloh, On polynomial invariants of several qubits, *J. Math. Phys.* **50**, 033509 (2009); The invariant-comb approach and its relation to the balancedness of multiple entangled states, *New J. Phys.* **12**, 075025 (2010).
- [26] A. Osterloh and J. Siewert, Entanglement monotones and maximally entangled states in multipartite qubit systems, *Int. J. Quantum Inf.* **04**, 531 (2006).
- [27] E. Jung and D. K. Park, Entanglement of four-qubit rank-2 mixed states, *Quantum Inf. Proc.* **14**, 3317 (2015).
- [28] T. J. Osborne and F. Verstraete, General Monogamy Inequality for Bipartite Qubit Entanglement, *Phys. Rev. Lett.* **96**, 220503 (2006).
- [29] Y.-K. Bai, D. Yang, and Z. D. Wang, Multipartite quantum correlation and entanglement in four-qubit pure states, *Phys. Rev. A* **76**, 022336 (2007).
- [30] Y.-K. Bai and Z. D. Wang, Multipartite entanglement in four-qubit cluster-class states, *Phys. Rev. A* **77**, 032313 (2008).
- [31] B. Regula, S. D. Martino, S. Lee, and G. Adesso, Strong Monogamy Conjecture for Multiqubit Entanglement: The Four-Qubit Case, *Phys. Rev. Lett.* **113**, 110501 (2014).
- [32] J. H. Choi and J. S. Kim, Negativity and strong monogamy of multiparty quantum entanglement beyond qubits, *Phys. Rev. A* **92**, 042307 (2015).
- [33] S. Karmakar, A. Sen, A. Bhar, and D. Sarkar, Strong monogamy conjecture in a four-qubit system, *Phys. Rev. A* **93**, 012327 (2016).
- [34] G. Vidal and R. F. Werner, Computable measure of entanglement, *Phys. Rev. A* **65**, 032314 (2002).
- [35] S. Lee, D. P. Chi, S. D. Oh, and J. Kim, Convex-roof extended negativity as an entanglement measure for bipartite quantum systems, *Phys. Rev. A* **68**, 062304 (2003).
- [36] A. Osterloh, J. Siewert, and A. Uhlmann, Tangles of superpositions and the convex-roof extension, *Phys. Rev. A* **77**, 032310 (2008).